

## APPLICATIONS OF MULTI-PHOTON MICROSCOPY IN CELL PHYSIOLOGY

Ernst Niggli and Marcel Egger

*Department of Physiology, University of Bern, B hlplatz 5, 3012 Bern, Switzerland*

### TABLE OF CONTENTS

1. Abstract
2. Introduction
  - 2.1. New possibilities
3. Functional imaging studies in living cells
  - 3.1. Calcium signaling
  - 3.2. Sodium and chloride signaling
  - 3.3. Two-photon imaging of metabolism
  - 3.4. Three-photon imaging of serotonin
  - 3.5. Green fluorescent protein and cameleons
4. Two-photon photolysis (TPP)
5. Problems that need to be addressed
6. Future developments
  - 6.1. Improved fluorescent indicators and caged compounds
  - 6.2. Fluorescence lifetime imaging (FLIM)
  - 6.3. Fluorescence resonance energy transfer (FRET)
  - 6.4. Entangled photon microscopy
7. Acknowledgments
8. References

### 1. ABSTRACT

Owing to its many optical and physical advantages for fluorescence excitation, multi-photon microscopy has found a wide range of uses in biology, both in structural and functional studies. In this review we highlight various applications of this technique in different fields of cell physiology and biophysical research. This includes studies on second messenger and ionic signals, on cellular metabolism as well as on genetically engineered probes and indicators. In addition, this technique has been successfully applied for diffraction-limited photolysis of caged compounds. We also point out some of the problems that were encountered along the still rapidly evolving path of this technique, and draw attention to some of the ongoing developments that will further extend and improve the usefulness of multi-photon excitation, such as fluorescence life-time imaging (FLIM), fluorescence resonance energy transfer (FRET) and entangled photon microscopy approaches.

### 2. INTRODUCTION

Immediately after the first report describing the application of multi-photon fluorescence excitation (MPE) for laser-scanning confocal microscopy (1, 2) many cell biologists and biophysicists recognized the immense potential of this new technique and a whole array of possible applications in living tissue and cells was envisaged. In the meantime, this technique has indeed found a wide range of uses, some of which we will summarize in this review. But we will also point out some of the unexpected difficulties that were encountered along the still evolving path of MPE

fluorescence microscopy. Finally, we would like to look into the future and speculate about upcoming developments that will without doubt further improve MPE technologies for applications in cell biology.

#### 2.1. New possibilities

From the physical and optical characteristics of multi-photon excitation one would reasonably foresee an extensive list of benefits when using MPE in physiological and biophysical studies. In this review, we will only briefly mention those that are particularly relevant when working with living tissue or cells. For more detailed information please refer to the review on the physical foundations of multi-photon excitation by David Piston, that will be published in this special issue of Frontiers in Bioscience.

1. As a rule of thumb the excitation wavelength is approximately doubled or tripled for two-photon and three-photon excitation, respectively. The strong wavelength-dependence of Rayleigh scattering should greatly improve the performance of laser-scanning inside scattering tissue (3) but also in large and thick single cells (e.g. skeletal muscle cells exhibiting diameters in the range of 100  $\mu\text{m}$ ).

2. The use of UV-lasers has remained difficult in confocal microscopy, mostly because of the absent or poor correction for axial and lateral chromatic aberration present in commercially available microscope objectives (4). Since most fluorescent indicators requiring UV excitation (for example Indo-1, Fura-2, SBFI, but also caged compounds) can be reasonably well excited with red or infra-red MPE,

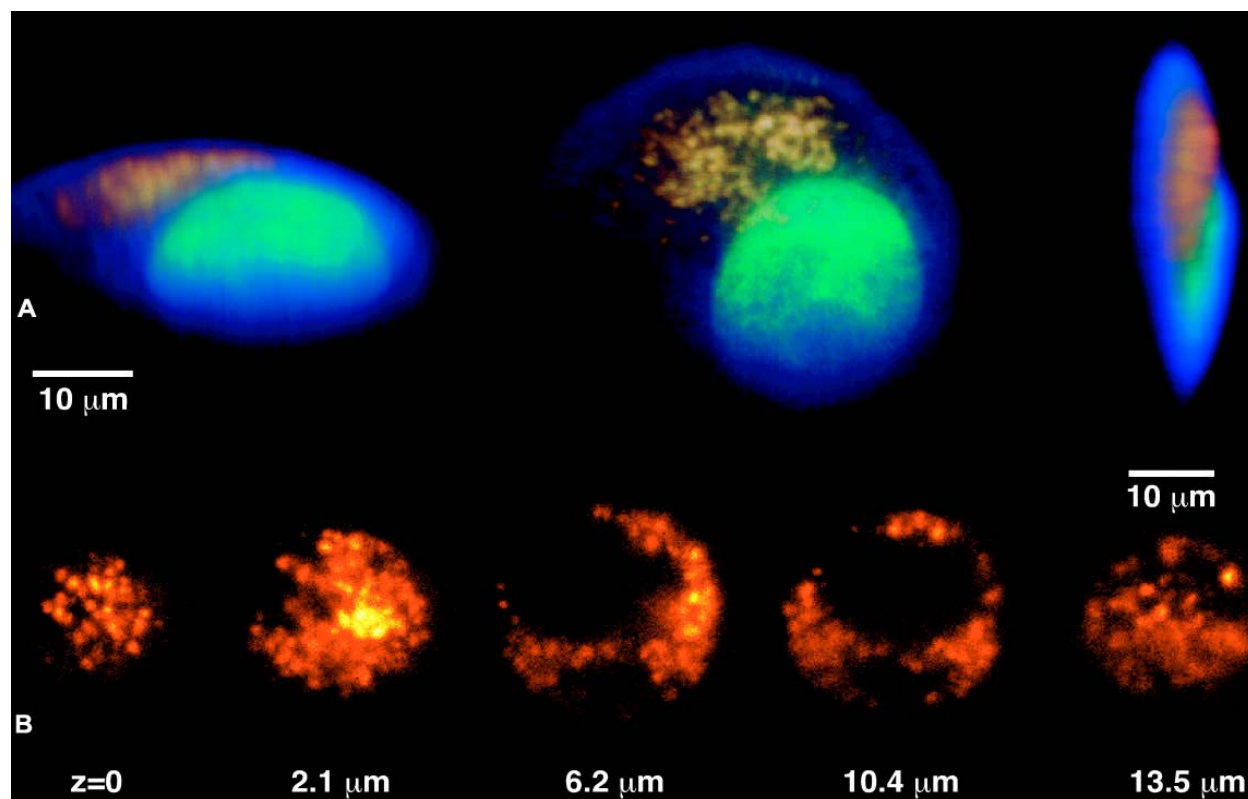


**Figure 1.** A: Three perspectives of a volume-rendered 3-D reconstruction of a live PC12 cell stained with acridine orange. The cell is shown from above (*center*), tilted by 60° along the horizontal axis (*left*) and rotated by 90° around the vertical axis (*right*). Acridine orange bound to nuclear DNA emits in the green (525 nm), whereas dye accumulated within acidic organelles generates fluorescence in the red (650 nm). Two-fluorescence channels were recorded. For the nuclei (green) a D520/60 interference filter was used, whereas the acidic organelles (red) were recorded with OG590 glass. In B: a sequence of slices through a typically shaped PC12 cell shows only the red component. While for the reconstruction in (A) each XY-slice was recorded within 200 ms, for the XY-slices in (B) only 75 ms exposure time was used. The images were recorded with a 60x water immersion objective; the excitation wavelength was 895 nm; the used total laser average power was 105 mW at the sample and was distributed to  $\approx 15$  foci. Reproduced (with permission) from Straub and Hell 1998.

the problems arising from chromatical aberration in the UV can be avoided with this technique.

3. In contrast to conventional single photon microscopy, excitation of the fluorescent indicator molecules only occurs in the focus of the illuminating laser beam, and thus exclusively in the focal plane. This feature leads to several interesting improvements when MPE is applied in living cells or tissue:

a. Both photobleaching and the cytotoxicity resulting from photoproducts of the fluorescent indicators are greatly reduced. This allows for longer experiment durations before cell damage occurs and thus also opens the door for the acquisition of three-dimensional datasets with laser-scanning, an application requiring a large number of confocal optical sections to be recorded (see Figure 1).

b. When using MPE even scattered photons are originating from the focal plane. This feature further improves imaging quality in turbid and scattering media, such as tissue and cells. In addition, scattered photons represent information

originating from the focal plane and can thus be collected to reconstruct the fluorescent image and to enhance detection efficiency with external detection devices.

c. Multiphoton excitation can also induce photolysis of caged compounds, which typically absorb strongly in the near UV. In contrast to UV-flash illumination, MPE of caged compounds will generate a diffraction limited point source of the biologically active photoreleased compound (for example calcium ( $\text{Ca}^{2+}$ ) or neurotransmitters). Therefore, this technique is ideal to probe cellular signaling systems on the subcellular level or to map the distribution of receptors for neurotransmitters in three-dimensional space.

### 3. FUNCTIONAL IMAGING STUDIES IN LIVING CELLS

#### 3.1. Calcium signaling

Changes of the intracellular  $\text{Ca}^{2+}$  concentration ( $[\text{Ca}^{2+}]_i$ ) are known to be a key event in many cellular signaling pathways and therefore of fundamental

importance in most cell types. Prominent and well studied  $\text{Ca}^{2+}$  activated mechanisms are, for example, excitation-contraction coupling in skeletal and cardiac muscle (5), pharmacomechanical coupling in smooth muscle (6), excitation-secretion coupling in secretory cells (7, 8) transmitter release and exocytosis (9) and synaptic plasticity (10). A variety of fluorescent  $\text{Ca}^{2+}$  indicators is available to record confocal  $\text{Ca}^{2+}$  images. Many laboratories have used the  $\text{Ca}^{2+}$  indicator Fluo-3 (and its latest derivatives) with great success. Fluo-3 has turned out to be the almost ideal fluorescent  $\text{Ca}^{2+}$  indicator for confocal microscopy because of its strong fluorescence signal, large dynamic range and its excitability by the 488 nm line of the Argon-ion lasers usually available on confocal instruments. Indeed, in several studies Fluo-3 has also been used with two-photon excitation, mainly to take advantage of the superior performance of this mode in thick specimens. In one example,  $\text{Ca}^{2+}$  signals were recorded from skeletal muscle cells loaded with Fluo-3 that was excited at 850 nm. This elegant study utilized the longitudinal structural periodicity of the muscle cell to increase the temporal resolution beyond the limit determined by the line-scan frequency (11). Using this approach, the authors could resolve and determine the expected diffusion delay for  $\text{Ca}^{2+}$  within the single sarcomeres (i.e. from the site of  $\text{Ca}^{2+}$  release near the T-tubules to the center of the sarcomere at the M-band, an event taking place within about 1 ms). This observation allowed to rule out the presence of a fast signal transduction mechanism for  $\text{Ca}^{2+}$  release inside the SR along the sarcomere.

Despite the superb quality of the fluorescence images obtained with Fluo-3 one disadvantage of this dye has always troubled investigators. Since Fluo-3 only exhibits a minimal shift of the emission spectrum upon  $\text{Ca}^{2+}$  binding, it cannot be used as a ratiometric  $\text{Ca}^{2+}$  dye (12). In many studies this is not of particular importance since only relative changes of  $[\text{Ca}^{2+}]_i$  are of interest and estimates of the  $\text{Ca}^{2+}$  concentrations are still possible with a self-ratio calibration procedure. However, in those experiments where the absolute  $\text{Ca}^{2+}$  concentration should be determined, ratiometric  $\text{Ca}^{2+}$  indicators would be a much better choice, since they can be calibrated for  $[\text{Ca}^{2+}]_i$  with fewer assumptions and thus more reliably. Unfortunately, all presently available ratiometric  $\text{Ca}^{2+}$  indicators, such as Indo-1 or Fura-2, require excitation by UV-light. As already mentioned, UV-confocal microscopes suffer from chromatic aberration problems. Therefore, it was an obvious strategy to try to excite Indo-1 with multiphoton techniques. Indo-1, which also changes its emission wavelength upon  $\text{Ca}^{2+}$  binding, has been widely used for quantitative recordings of  $\text{Ca}^{2+}$ , while Fura-2 has been preferred for imaging as a dual excitation single emission ratiometric  $\text{Ca}^{2+}$  indicator. For confocal microscopy where multiple detectors are usually available, the single excitation dye Indo-1 has found several applications. For example in a study of  $\text{Ca}^{2+}$  waves in keratocytes induced by strong electrical depolarization (13) and in a paper describing  $\text{Ca}^{2+}$  signals in cardiac myocytes (14). In the latter study an interesting observation was made: with two-photon excitation (at 705 nm) the isosbestic emission

wavelength of Indo-1 appeared to be shifted towards shorter wavelengths by about 40 nm. As it turned out, this effect was resulting from an unexpectedly small two-photon absorbance of Indo-1 that prevailed when the dye molecules had  $\text{Ca}^{2+}$  bound. Unfortunately, this drawback of Indo-1 limits its usefulness for  $\text{Ca}^{2+}$  measurements with MPE since the signal available from the shorter emission wavelength (i.e. around 400 nm) is greatly reduced (see also paragraph on “Problems” and “Future Developments”).

Another ongoing development aims to target fluorescent indicators to specific subcellular locations that may be much smaller than the optical resolution of laser-scanning confocal microscopes. Since fluorescence can be detected even if it originates from a structure that is below the diffraction limit (in fact even from a single molecule), fluorescence signals can be attributed to very specific locations once the dyes can be specifically targeted. Earlier attempts to implement this strategy used lipid-conjugated  $\text{Ca}^{2+}$  sensitive indicators such as FFP-18 (the C18-Fura-2 derivative), FIP-18 (the C18-Indo-1 conjugate) and C-18- $\text{Ca}^{2+}$ -green, all of which can be excited with MPE (see Figure 2A for two-photon excitation image of cultured cardiac myocyte loaded with FIP-18). With this strategy it has been possible to record  $\text{Ca}^{2+}$  signals originating from spaces very close to the cell membrane (15, 16). Interestingly, during  $\text{Ca}^{2+}$  fluxes across the membrane these signals were significantly different in both amplitude and time course from those measured in the bulk of the cytosol, suggesting the existence of  $\text{Ca}^{2+}$  concentration gradients near the plasmalemma. Such gradients are assumed to be very important, since the proteins located in the cell membrane, such as ion channels or transporters, are likely to “see” this local ion concentration and not the average cytosolic  $[\text{Ca}^{2+}]_i$  that is commonly measured. In combination with molecular biology engineering techniques the idea of targeted ion indicators has recently been taken one step further, as described below.

A fair number of papers have been published during the last few years describing the application of MPE to examine  $\text{Ca}^{2+}$  signaling in neuronal cells, dendrites and spines. A detailed account of this work can be found in the chapter on MPE applications in the neurosciences by Cruz & Lüscher, published in this special issue of *Frontiers in Bioscience*.

### 3.2. Sodium and chloride signaling

While many spatial features of cellular  $\text{Ca}^{2+}$  signals have been investigated with imaging techniques in great detail, the functional importance of the intracellular  $\text{Na}^+$  concentration and its distribution is less clear. It is generally appreciated that in many cell types the cytosolic  $\text{Na}^+$  concentration ( $[\text{Na}^+]_i$ ) is tightly linked to  $[\text{Ca}^{2+}]_i$  and pH<sub>i</sub> via the Na-Ca exchange and the Na-H exchange mechanism, respectively. Both transporters use the electrochemical  $\text{Na}^+$  gradient across the cell membrane as their energy source. In cardiac muscle the cytosolic  $\text{Na}^+$ -concentration is known to strongly affect the contractile state (17). In fact, cardiotonic steroids such as ouabain are believed to strengthen the heart beat by initially inhibiting

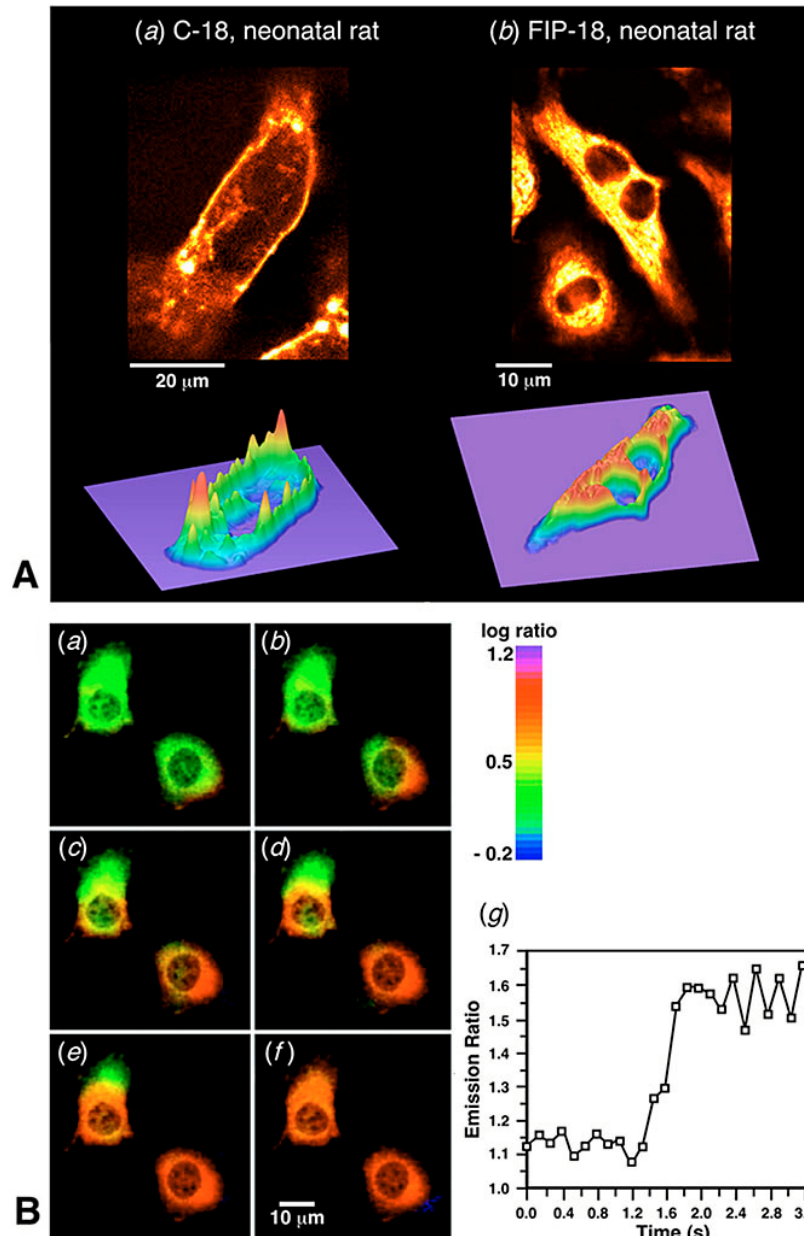


**Figure 2.** A: Cellular staining with lipid-conjugated fluorescent  $\text{Ca}^{2+}$  indicators for near-membrane measurements of  $[\text{Ca}^{2+}]$ . A cultured neonatal rat myocyte stained by extracellular application of Calcium-Green-1 (the lipid-conjugate of the indicator Calcium-Green-1; 5  $\mu\text{M}$ , 60 min) and the corresponding surface plot are shown in (Aa). The cell depicted in (Ab) had been exposed to FIP-18 (the lipid-conjugate of the ratiometric UV indicator Indo-1; 5  $\mu\text{M}$ , 60 min). FIP-18 was excited with a two photon excitation system (mode-locked Ti:sapphire laser: Mira 900-F, Coherent; pulse duration:  $\approx 75$  fs, 705 nm, 10-30 mW). The fluorescence emission was recorded at  $>460$  nm with a laser-scanning confocal microscope (MRC1000, BioRad). FIP-18 distributed throughout the entire cell with the exception of the nuclear region. In contrast, the C-18 fluorescence pattern (excitation 488 nm, emission  $> 525$  nm) showed a clear outline of the cell membrane. The rapid fluorescence response to changes of extracellular  $\text{Ca}^{2+}$  and the ability to maximally quench the C-18 fluorescence by extracellular  $\text{Ni}^{2+}$  indicated that C-18 was incorporated into the outer leaflet of the cell membrane with the  $\text{Ca}^{2+}$ -sensing fluorophore oriented towards the extracellular space (for additional information see (16)). B: Video-rate scanning two-photon excitation fluorescence microscopy and ratio imaging with cameleons. (a-f) Ratio imaging (535/480 nm) of a  $\text{Ca}^{2+}$  wave in HeLa cells expressing a cytosolic cameleon without targeting signals. The calcium wave (red) was created with the application of 0.1 mM histamine, which triggers  $\text{Ca}^{2+}$  release in the cells, and can be seen to propagate across each cell. Images (a) and (f) were recorded 1 s before and 6 s after the application of histamine, respectively. The interval between images (b-e) is 132 ms. (g) Time course of average  $\text{Ca}^{2+}$  in HeLa cells associated the application of histamine, measured from the cytoplasm. Reproduced (with permission) from (39).

the Na-K-ATPase which results in a subsequent elevation of  $[Na^+]_i$ . This rise of  $[Na^+]_i$  ultimately changes the reversal potential for the Na-Ca exchange, leading to an increase of the  $Ca^{2+}$  content of the sarcoplasmic reticulum and larger  $Ca^{2+}$  transients.

Recently, a more direct effect of  $Na^+$  entry into cardiac muscle cells has been proposed to occur during EC-coupling. Despite the tiny change of the average  $[Na^+]_i$  that would result from a single activation of the  $Na^+$  current, it was observed that this small amount of  $Na^+$  entering the cell could activate the Na-Ca exchange to run in the  $Ca^{2+}$  influx mode which then triggered  $Ca^{2+}$  release from the SR (18, 19). Estimates of the  $Na^+$  signals resulting from a single activation of the  $Na^+$  current suggested an increase of  $[Na^+]_i$  from 8 mM to only about 8.05 mM, a change that was certainly not sufficient to affect the Na-Ca exchange significantly. Therefore, the existence of a subsarcolemmal space has been proposed from which escape of  $Na^+$  ions by diffusion would be restricted ("fuzzy space"; (20).

Within this small volume presumably corresponding to the dyadic cleft space, changes of  $[Na^+]_i$  would of course be much more pronounced and sufficient to briefly activate the Na-Ca exchange in the  $Ca^{2+}$  influx mode. Thus, microdomains of large concentration gradients for  $[Na^+]_i$  have been implied quite some time ago but their direct experimental visualization is still lacking. Interestingly, using electron probe microanalysis of  $Na^+$ , spatially larger gradients have been found to exist in guinea-pig ventricular myocytes during the period of  $Ca^{2+}$  removal via Na-Ca exchange (21), and very recently also in a confocal microscopic study using multi-photon excitation of the  $Na^+$  indicator SBFI (see (22) and the review by Kockskämper *et al.* in this special issue of Frontiers in Bioscience).

SBFI is a ratiometric  $Na^+$  indicator with spectral properties very similar to Fura-2 (23). Thus, it is an excitation ratiometric dye and for two-photon studies would ideally be excited with two different wavelengths (24). To achieve adequate temporal resolution this would require the use of a pair of rapidly alternating two-photon excitation laser systems, equipment that is not readily available. However, SBFI can also be used as a single excitation single emission wavelength indicator, although the recordings will then no longer be ratiometric.

In cell types which have high surface-to-volume ratios, significant changes of  $[Na^+]_i$  would be expected to occur after eliciting a few sodium currents. An extraordinary example are dendrites, spines and axons of neurons, where the presence of  $Na^+$  permeable membrane channels is combined with an extremely small cytosolic volume. Large changes of  $[Na^+]_i$  were indeed observed in spines and dendrites during experiments where the whole-cell variant of the patch-clamp technique was combined with two-photon excitation of SBFI (at 790 nm; (25, 26)). To account for the limitations of the non-ratiometric use of the dye and to obtain a more quantitative signal a calibration of SBFI for  $Na^+$  was performed after each experiment. A short burst of action potentials increased the

$[Na^+]_i$  within active spines from 10 mM to about 20 mM while a prolonged stimulation (100 Hz for 1 second) led to an increase up to 100 mM. This local signal was restricted to a dendritic domain near the site of synaptic input (see Figure 3; (26)).

### 3.3. Two-photon imaging of metabolism

Autofluorescence of the cells represents a significant experimental difficulty, particularly when working with fluorescent indicators requiring excitation with UV-light. A substantial fraction of the autofluorescence arises from the presence of NADH, an intermediate of the cellular metabolism. Taking advantage of this endogenous indicator a number of fluorescence spectroscopic and imaging studies have been carried out to examine changes of the metabolic state in individual cardiac and skeletal muscle cells when imposing a variety of stresses or adding poisons, such as cyanide (for example see (27-31)). Using two-photon excitation of rabbit cornea three-dimensional maps of the cellular metabolic state have been obtained throughout the entire thickness of 400  $\mu m$  (32). The autofluorescence was confirmed to be mostly of NADH origin by cyanide exposure, which increased the fluorescence from all cell types in the cornea by about a factor of two. Using the same experimental approach, NADH was quantified in two subcellular compartments, the cytosol and mitochondria of  $\beta$ -cells within cultured pancreatic islets (33). With the spatial resolution of two-photon confocal imaging it was found that the stimulation of the two compartments occurred with different kinetics. Taken together, two-photon microscopy appears to be an ideal technique for studies requiring imaging of cellular and subcellular metabolic states.

### 3.4. Three-photon imaging of serotonin

Another example where endogenous compounds were used as fluorescent indicators for confocal microscopy was published a few years ago (34). In this study, a Ti:sapphire laser running at a wavelength of 700 nm was applied for three-photon excitation of serotonin. Fluorescence images were recorded from rat basophilic leukemia cells (RBL cells) that had been incubated in serotonin for several hours. Serotonin is actively transported into these cell and finally concentrated into secretory granules that could be visualized. Immunogenic stimulation of the RBL cells leads to a reaction of degranulation that could be followed as a marked reduction of the punctate features.

### 3.5. Green fluorescent protein and cameleons

The green fluorescent protein (GFP) from the jellyfish *Aequorea victoria* rapidly found widespread application as an efficient intracellular fluorophore, particularly when expressed as a tag on a fusion protein (for reviews see (35, 36)). Examples are studies of cytoskeletal structure and cell division, organelle dynamics with targeted proteins, protein localization and many others. Several classes of mutants of GFP have been engineered exhibiting distinct differences in their excitation and emission spectra, but also in their rate of photobleaching and pH sensitivity. An especially promising development

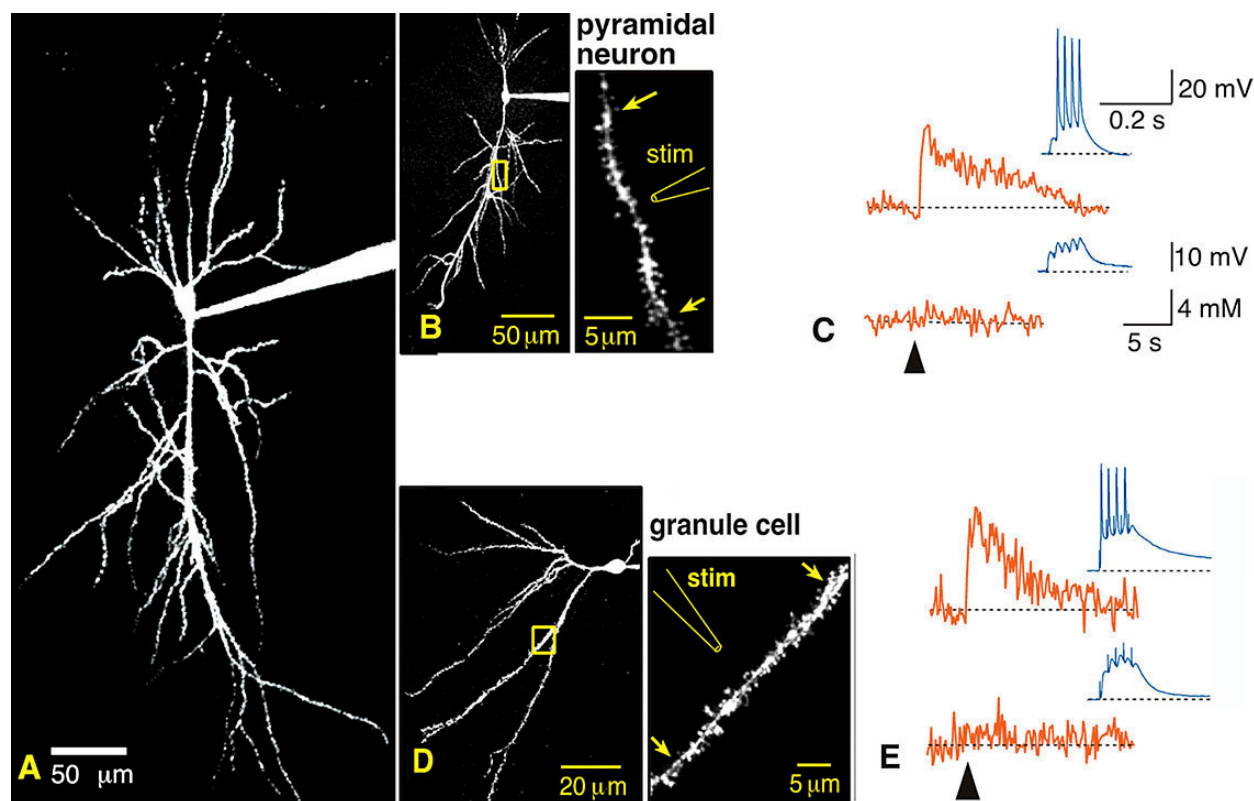


**Figure 3.** Two-photon excitation of sodium-binding benzofuran-isophthalate (SBFI). (A) Montage of a stack of 29 optical sections taken at 5  $\mu\text{m}$  intervals through a CA1 pyramidal neuron filled with 2 mM SBFI. (B, left)  $\text{Na}^+$  transients require suprathreshold stimulation. Reconstruction of a stack of 24 optical sections taken at 5  $\mu\text{m}$  intervals through an SBFI-filled CA1 pyramidal cell. The box indicates the area enlarged in the right panel showing a spiny dendrite from the same cell taken at higher z-resolution (0.4  $\mu\text{m}$ ). The position of the stimulation electrode is indicated schematically. The arrows point to the dendritic region from which measurements in (C) were obtained. (C) Suprathreshold synaptic stimulation (top traces) induced a prominent  $\text{Na}^+$  transient in the dendrite, whereas subthreshold stimulation (bottom traces) did not result in a measurable  $\text{Na}^+$  increase. (D, left) Stack of 20 optical sections (3.5  $\mu\text{m}$  intervals) through a granule cell of the dentate gyrus filled with SBFI. The box indicates the area enlarged on the right showing a spiny dendrite from the same cell (z-step 0.7  $\mu\text{m}$ ). The arrows indicate the dendritic region from which measurements in (E) were obtained. (E) Suprathreshold stimulation evoked a  $\text{Na}^+$  transient in the dendrite (top traces). Subthreshold stimulation, in contrast, did not result in a  $\text{Na}^+$  transient (bottom traces). Arrowheads in C and E indicate the time of synaptic stimulation. Calibration for E is shown in C. Reproduced (with permission) from (25, 26).

are tandem fusion proteins containing a blue-emitting mutant GFP and a green- or yellow-emitting GFP, both linked together with calmodulin (37). These constructs are termed “cameleons” and show fluorescence resonance energy transfer (FRET) which is enhanced when calmodulin binds  $\text{Ca}^{2+}$  (see Figure 2B). Thus,  $\text{Ca}^{2+}$  binding leads to an increase in the green emission while the blue emission is reduced, a feature which allows for ratiometric calibration. Since these proteins can be expressed *in situ* they could be efficiently targeted to subcellular organelles such as the nucleus, mitochondria or the endoplasmic reticulum (38). By mutating the linking calmodulin, the  $\text{Ca}^{2+}$  sensitivity has been adjusted to meet the concentrations prevailing in the targeted organelle.

Several studies have now already been performed where the advantages of these fluorescent indicators have been combined with MPE (for example

see (39)). The combination of these two techniques has obvious advantages when the fate of cells should be followed over long periods of time and in three dimensions in developing embryos (of growing size and thickness). As  $\text{Ca}^{2+}$  indicators the cameleons have the enormous potential to be specifically targeted to organelles, thus allowing  $\text{Ca}^{2+}$  measurements from these small spaces. They might even be targeted to specific proteins possibly enabling  $\text{Ca}^{2+}$  measurements from spaces that are too small to be resolved because of the limits arising from optical diffraction.

#### 4. TWO-PHOTON PHOTOLYSIS (TPP)

As already mentioned, with multi-photon techniques the excitation of fluorescent molecules only occurs in a diffraction limited volume. This feature of multi-photon excitation not only results in reduced



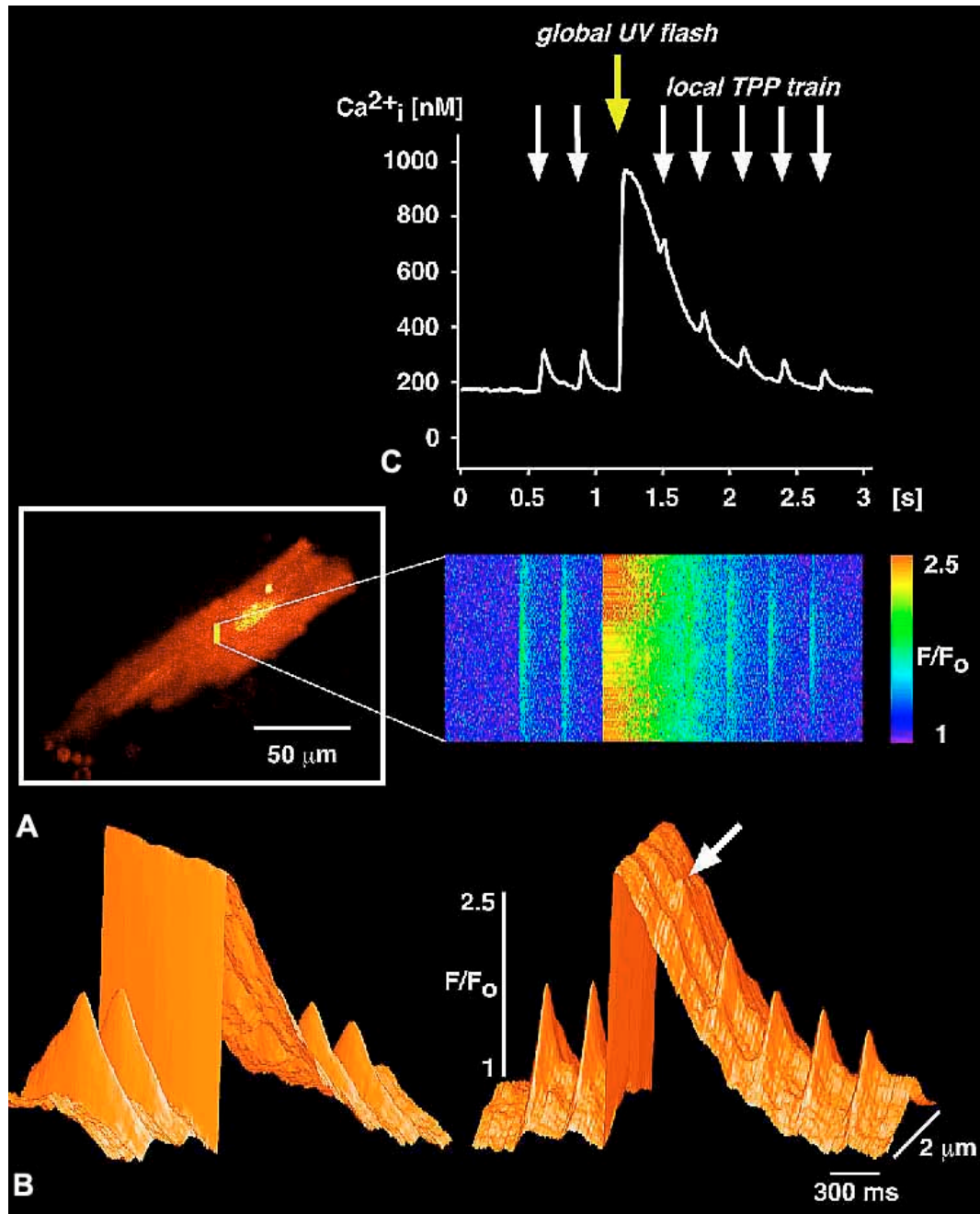


**Figure 4.** Confocal  $\text{Ca}^{2+}$  images of local two-photon-photolytic  $\text{Ca}^{2+}$  signals (TPP) in combination with a global  $\text{Ca}^{2+}$  release signals induced by UV-flash photolysis. (A) Left inset, confocal image showing Fluo-3 fluorescence in a ventricular myocyte. The vertical yellow line indicates the line that was scanned repetitively at 500 Hz to record the line-scan image (right). Intracellular local  $\text{Ca}^{2+}$  signals were elicited by two-photon photolysis of DM-nitrophen (average power at microscope camera port: 70 mW; TPP shutter opening: 30 ms, interval: 400 ms). The color scale bar shows pseudo-ratio values ( $F/F_0$ ) corresponding to resting (purple) and elevated (red)  $\text{Ca}^{2+}$  concentration. (B) Surface plot computed from the line-scan image shows two TPP signals of equal amplitude preceding a global  $\text{Ca}^{2+}$  signal elicited by UV-flash photolysis of caged  $\text{Ca}^{2+}$ . The first TPP signal after the global signal was markedly suppressed (arrow), thus global  $\text{Ca}^{2+}$  release signals inhibit subsequent local events but not vice versa. (C) In spatially averaged temporal  $\text{Ca}^{2+}$  profiles extracted from the line-scan, the depression and gradual recovery of the TPP signals becomes obvious. After the global signal all local signals show a reduction in amplitude, presumably resulting from photoconsumption of DM-nitrophen during the whole-cell flash (for details see (52)).

photobleaching of fluorescent indicators but can, in principle, also be utilized to create subcellularly targeted point-sources of biologically active substances by photorelease from caged compounds that normally require UV light for excitation. Subcellular spatial targeting of messengers has recently been recognized as a means by which cells can encode information and prevent cross-talk between different signaling pathways (for example for cAMP (40), for  $\text{Ca}^{2+}$  (41)). Caged compounds exist for a growing range of biologically active substances including, for example, neurotransmitters, second messengers, metabolic substrates and ions (for review see (42)). UV-flash photolysis has significant advantages over other experimental approaches to change concentrations. Most importantly, the photolytic liberation is a very fast process ( $\mu\text{s}$  to  $\text{ms}$ ) that is not kinetically limited by diffusion. This advantage is particularly striking when the concentration of a substance needs to be changed inside a living cell. Two-photon excitation now adds a new twist to these photolytic techniques. When combining photolytic experimental strategies with this approach, the experimenter achieves direct control over the location of photorelease in three-dimensional space (with  $\mu\text{m}$  precision). Of course, the photoreleased substance will immediately start to diffuse away from the diffraction limited site of release, a process which can somewhat degrade the spatial precision. Making use of these possibilities, two-photon excitation of caged compounds has been efficiently exploited to address a number of questions. In one study, spatially defined photorelease of an agonist has been applied to map the location and distribution of nicotinic acetylcholine receptors on the surface of cultured BC3H1 cells using a photoactivatable precursor of carbamoylcholine (43). In principle, the same approach could be used to map any other type of receptors for which caged agonists are available or will be developed in the future (44-46).

Several studies have been carried out to probe  $\text{Ca}^{2+}$  signaling in cardiac muscle cells on the subcellular level with a caged compound. In this application the two-photon photolysis has turned out to be a valuable tool since it allowed to mimic and examine some features of spatially limited elementary events of  $\text{Ca}^{2+}$  signaling,  $\text{Ca}^{2+}$  quarks and  $\text{Ca}^{2+}$  sparks. This technique is especially valuable when combined with confocal imaging of the resulting  $\text{Ca}^{2+}$  signals (47, 48).  $\text{Ca}^{2+}$  quarks and sparks are thought to arise from the opening of either a single channel or a group of intracellular  $\text{Ca}^{2+}$  release channels located on the  $\text{Ca}^{2+}$  store of muscle cells, the sarcoplasmic reticulum (SR; (49, 50)). Thus,  $\text{Ca}^{2+}$  quarks and sparks represent the building blocks of  $\text{Ca}^{2+}$  signaling and excitation-contraction coupling in muscle (41). When performing stationary two-photon photolysis of the caged  $\text{Ca}^{2+}$  compound DM-nitrophen (excited at 710 nm) while simultaneously imaging the  $[\text{Ca}^{2+}]_i$  with the fluorescent  $\text{Ca}^{2+}$  indicator Fluo-3 (excited at 488 nm), our laboratory has been able to show that  $\text{Ca}^{2+}$  release events smaller than  $\text{Ca}^{2+}$  sparks indeed can be elicited in isolated cardiac myocytes, possibly corresponding to the  $\text{Ca}^{2+}$  quarks that, by our definition, result from the opening of a single SR  $\text{Ca}^{2+}$  release channel

(also termed Ryanodine receptor or RyR (47)). The existence of  $\text{Ca}^{2+}$  release events smaller than  $\text{Ca}^{2+}$  sparks had previously been suggested based on the observation of  $\text{Ca}^{2+}$  release transients triggered by UV-flash photolysis of caged  $\text{Ca}^{2+}$  that contained no resolvable  $\text{Ca}^{2+}$  sparks (51). More recently, repetitive applications of UV-laser flashes or pairs of TPP pulses also allowed to distinguish between several possible mechanisms underlying a period of refractoriness of  $\text{Ca}^{2+}$  release from the  $\text{Ca}^{2+}$  store (52). Interestingly, long lasting refractoriness (similar to 1 second) was only observed when many RyRs were activated simultaneously, i.e. with UV-flashes illuminating the entire cell. However, local activation of a small number of RyRs by TPP did not induce this refractoriness. A significant  $\text{Ca}^{2+}$  depletion of the  $\text{Ca}^{2+}$  store, which does not occur after local activation of  $\text{Ca}^{2+}$  release, could explain this apparent discrepancy. Taken together, by allowing a direct comparison between the highly localized behavior of the  $\text{Ca}^{2+}$ -induced  $\text{Ca}^{2+}$  release system with the global cellular response, two-photon photolysis has revealed fundamental features of a biological cellular process.

When testing various caged compounds it soon turned out that not all do respond equally well to multi-photon excitation with near-infra red light ( $\approx 700 \text{ nm}$ ). Many compounds have very small two-photon absorbance cross sections. As a result of this, the power levels required to obtain sufficient photolysis is close to or even above the limits tolerated by living cells. For example, it was found that the caged  $\text{Ca}^{2+}$  compound DM-nitrophen produced much larger signals than the similar compound NP-EGTA (53). Since NP-EGTA has a better specificity for  $\text{Ca}^{2+}$  over  $\text{Mg}^{2+}$  than DM-nitrophen, an attempt was made to combine the larger two-photon absorbance of the di-methoxy caging group with the  $\text{Ca}^{2+}$  specificity of NP-EGTA. The resulting compound, DMNPE-4 has been successfully used to generate  $\text{Ca}^{2+}$  transients and local TPP  $\text{Ca}^{2+}$  signals despite the presence of a physiological or even elevated concentration of  $\text{Mg}^{2+}$ , whereas no  $\text{Ca}^{2+}$  release could be detected from DM-nitrophen under these conditions (i.e. presumably only  $\text{Mg}^{2+}$  release occurred (54).

After the small absorbance cross section of many caged compounds and fluorescence indicators had been revealed, developments were undertaken to create new caging groups with greatly improved absorbance for TPP. Some of this ongoing work will be briefly described below and in more detail in the review by Ellis-Davies *et al.* in this issue.

## 5. PROBLEMS THAT NEED TO BE ADDRESSED

As with most other newly introduced biophysical techniques, multi-photon excitation was initially greeted with a high degree of enthusiasm. But during the years of development and experimentation, several problems surfaced that have somewhat limited the widespread application but also, at least in the biomedical field, the experimental yield of this technique. The most important obstacle to the more popular use of MPE is, without any doubt, the still very high price tag on the ultrafast laser systems. With the recent commercial introduction of



several turn-key solid-state lasers, the costs and the complexity for such a system have decreased somewhat and one might expect more change on the price front in the foreseeable future. But also those laboratories which already have installed multi-photon excitation lasers face several problems and observe side-effects arising from the high peak power levels required for sufficient two- or three-photon excitation, problems that are of course of vital importance when working with living cells. Interestingly, many of the reported problems seem to have a single common cause: a less than ideal two-photon absorbance cross section of presently available and frequently used fluorescent indicators and caged compounds (55). Even on a perfectly aligned confocal microscope, that may be equipped with an external photon detection device (to collect the confocal information present in scattered photons), this limitation of the fluorophore requires the use of fairly high excitation power levels that may have several side-effects in cells. Extremely high power levels can lead to immediate cell death, probably resulting from puncture of the cell membrane. At power levels that are typically used to excite fluorescent indicators with two-photon techniques (average power 1 - 10 mW on the cell) several adverse effects have been observed and reported (56, 57). When exciting various  $\text{Ca}^{2+}$  indicators at 870 nm in dendrites of pyramidal neurons, photodamage was noticed as irreversible changes of the fluorescence  $\text{Ca}^{2+}$  signal and the duration of an experiment was limited by phototoxic effects (56). At low excitation power, photodamage appeared to accumulate linearly with exposure time. The findings after variation of the laser pulse length suggested, that a two-photon mechanism was mainly responsible for the cumulative damage. However, it has recently been pointed out that this type of photodamage may be a threshold phenomenon that only occurs above a specific power level. When two different biological indicators of damage (changes in resting  $[\text{Ca}^{2+}]_i$  and the degranulation reaction) were recorded in bovine adrenal chromaffin cells, damage was found to be proportional to the integral (over space and time) of light intensity raised to a power of approximately 2.5 (58). This may indicate that the damaging events not only arise from two-photon excitation of the  $\text{Ca}^{2+}$  indicator but may include higher order processes, such as three-photon photodestruction of cellular constituents (and thus may arise from the high peak power prevailing during each 100 fs pulse).

Whatever the nature of the underlying damaging processes might be, it appears that the amount and time-course of photo-injury is critically dependent on the experimental conditions. The design of a particular experiment also defines how much and what type of photodamage can be accepted. For example, a study of  $\text{Ca}^{2+}$  signaling performed on single cells will not be limited by any ruptures of the nuclear DNA. But such a side effect would render long lasting developmental studies on the same preparation impossible. Thus, the problem is particularly pronounced in long-term recordings from living tissue. In one example, where the dynamics of mitochondrial distribution were monitored in hamster embryos over 24 h using two-photon microscopy of the dye Mitotracker-X-Rosamine (excitation at 1,047 nm), the fetal developmental

competence was fully maintained (59). In contrast, single-photon confocal imaging of the same preparation for only 8 h inhibited further development, even when no fluorophore was added. Thus, two-photon microscopy, but not confocal microscopy, has permitted long-term fluorescence in highly photosensitive specimens such as mammalian embryos.

Taken together, it is presently not yet clear, exactly what mechanisms are responsible for the reported side-effects. Most likely, a range of experimental parameters is important, including the dye, the wavelength (absorption by water) and power of excitation (average and peak power). However, it appears obvious that difficulties mentioned above could be greatly alleviated with newly developed fluorescent indicators that exhibit large two-photon absorption cross-sections (see below).

## 6. FUTURE DEVELOPMENTS

Improvements and further developments of multi-photon excitation systems are presently under way. This includes the search for new fluorescent indicators and caged compounds. In addition, the combination of MPE with techniques other than fluorescence intensity imaging may offer unique opportunities to peek into the functioning of living cells.

### 6.1. Improved fluorescent indicators and caged compounds

In several laboratories the search for fluorophores exhibiting large two-photon absorbance cross sections has been initiated and promising compounds have already been reported. So far, no or very few indicators or caged compounds based on these highly absorbing fluorophores are commercially available, such as a new caged glutamate based on a brominated 7-hydroxycoumarin-4-ylmethyl ester (for examples see (44, 60, 61). But this situation is expected to ameliorate in the near future. A related strategy involves improving the two-photon absorbance by slightly modifying already existing compounds. As already mentioned above, DMNPE-4 was developed based on such a strategy (54). Similarly, DMCNB-glutamate and MNI-glutamate were engineered with the goal to exhibit a sufficiently large two-photon cross-section and were used to map the distribution of glutamate receptors on cultured hippocampal neurons (45). When several already available caged compounds were screened for two-photon absorbance, it turned out that Azid-1 exhibited an almost 100-fold larger absorbance cross section than DM-nitrophen (62). Unfortunately, the  $\text{Ca}^{2+}$  affinity of Azid-1 ( $K_d = 230$  nM) is not as high as that of DM-nitrophen ( $K_d = 5$  nM), which limits its use in cells that do not allow their resting  $[\text{Ca}^{2+}]_i$  to be elevated to pre-load the caged compound with  $\text{Ca}^{2+}$ .

A new and promising class of fluorescent indicators are quantum dot nanocrystals which exhibit very large two-photon absorbance cross-sections (63) and may find research applications in cell physiology (64, 65).

### 6.2. Fluorescence lifetime imaging (FLIM)

A well known problem of quantitative fluorescent indicators is their uneven distribution inside cells. This

mainly results from compartmentalization into subcellular organelles but also from binding of the dyes to intracellular constituents, such as proteins and lipids (66). The inhomogeneous distribution is manifest as local non-uniformities in fluorescence intensity. Ratiometric indicators provide an easy way to correct for a majority of the artifacts arising from the inhomogeneous dye distribution, since the ratio is obtained by dividing two fluorescence intensities recorded at two different wavelengths. By dividing the two fluorescence images the concentration of the dye cancels out. Interestingly, many fluorescent indicators not only alter the intensity of their emission after binding their substrate but also undergo a change of the fluorescence lifetime (see also (2)). Intrinsically, the fluorescence life-time is dependent on many factors in the environment of the dye molecules but independent of dye concentration. Based on this concept several instruments have been developed to image fluorescence life-time distribution (e.g. (67)), lately also making use of two-photon excitation (68, 69). FLIM may therefore be a valuable addition to MPE, also to exploit features of dyes that are not manifest as changes of quantum yield or absorbance, both resulting in changes of emitted fluorescence intensity. In fact, dyes specifically designed for large changes of fluorescence lifetime might become a new tool in the future.

### 6.3. Fluorescence resonance energy transfer (FRET)

FRET uses two matched fluorescent indicators where the emission spectrum of the shorter wavelength dye (donor) overlaps with the absorption spectrum of the acceptor dye (70). Radiationless energy transfer occurs only when the donor and acceptor are in close proximity. The efficiency of FRET depends on the distance between the two molecules raised to the power of 6. Therefore, this technique is extremely useful for co-localization studies. Since FRET operates in the range of Angstroms it is several orders of magnitude more sensitive than conventional co-localization by imaging, which has a resolution that is essentially determined by the optical diffraction limit. A promising variant of FRET is offered by the possibility to link two fluorescent molecules with a third compound that undergoes a conformational change upon binding of a substrate. When this conformational rearrangement is associated with a change of the distance between the two fluorophores, a change of the FRET efficiency is expected. Such a strategy could be used to engineer novel fluorescent indicators, such as the “cameleons” mentioned above (36).

### 6.4. Entangled photon microscopy

Several groups are theoretically and experimentally investigating the entanglement (71) of two-photon states generated via pulse-pumped parametric down-conversion of light (72, 73)). Quantum entanglement is a phenomenon that allows a quantum state to be teleported over large distances almost instantaneously (i.e. faster than the speed of light). Photons generated with this technique are correlated both in time and space and therefore absorption no longer depends on an accidentally simultaneous arrival of two photons. Therefore, the rate of two-photon absorption no longer quadratically depends in photon flux density, but instead appears to be linear. These features would yield important improvements

over conventional MPE. (1) Two-photon absorbance is expected to be much better, possibly approaching that of single photon absorption. (2) Power levels required for two-photon excitation may be dramatically reduced, coming close to those for single photon excitation. (3) Spatial resolution would be improved since two-photon excitation would only occur in a volume in which correlated photon pairs overlap in space and time. While this technique has not yet been implemented as a functional confocal microscope, it sure looks quite promising and ongoing developments should be highly interesting.

## 7. ACKNOWLEDGEMENTS

This work was supported by grants from the Swiss National Science Foundation, the Swiss Cardiac Research and Training Network and the Swiss Federal Office for Science and Education.

## 8. REFERENCES

1. Denk, W., J. H. Strickler & W. W. Webb: Two-photon laser scanning fluorescence microscopy. *Science* 248, 73-76 (1990)
2. Pawley, J. B: Handbook of biological confocal microscopy. 2nd Edn. Plenum Press. New York (1995)
3. Centonze, V. E. & J. G. White: Multiphoton excitation provides optical sections from deeper within scattering specimens than confocal imaging. *Biophys J* 75, 2015-2024 (1998)
4. Niggli, E., D. W. Piston, M. S. Kirby, H. Cheng, D. R. Sandison, W. W. Webb & W. J. Lederer: A confocal laser scanning microscope designed for indicators with ultraviolet excitation wavelengths. *Am J Physiol* 266, C303-310 (1994)
5. Bers, D. M: Excitation-contraction coupling and cardiac contractile force. 2nd Edition. Kluwer. Dordrecht, Netherlands (2001)
6. Somlyo, A. P. & A. V. Somlyo: Signal transduction and regulation in smooth muscle. *Nature* 372, 231-236 (1994)
7. Thorn, P., A. M. Lawrie, P. M. Smith, D. V. Gallacher & O. H. Petersen: Local and global cytosolic  $\text{Ca}^{2+}$  oscillations in exocrine cells evoked by agonists and inositol trisphosphate. *Cell* 74, 661-668 (1993)
8. Maruyama, Y., G. Inooka, Y. X. Li, Y. Miyashita & H. Kasai: Agonist-induced localized  $\text{Ca}^{2+}$  spikes directly triggering exocytotic secretion in exocrine pancreas. *Embo J* 12, 3017-3022 (1993)
9. Zucker, R. S: Exocytosis: A molecular and physiological perspective. *Neuron* 17, 1049-1055 (1996)
10. Cummings, J. A., R. M. Mulkey, R. A. Nicoll & R. C. Malenka:  $\text{Ca}^{2+}$  signaling requirements for long-term depression in the hippocampus. *Neuron* 16, 825-833 (1996)

11. Hollingworth, S., C. Soeller, S. M. Baylor & M. B. Cannell: Sarcomeric  $\text{Ca}^{2+}$  gradients during activation of frog skeletal muscle fibres imaged with confocal and two-photon microscopy. *J Physiol* 526, 551-560 (2000)
12. Minta, A., J. P. Kao & R. Y. Tsien: Fluorescent indicators for cytosolic calcium based on rhodamine and fluorescein chromophores. *J Biol Chem* 264, 8171-8178 (1989)
13. Brust-Mascher, I. & W. W. Webb: Calcium waves induced by large voltage pulses in fish keratocytes. *Biophys J* 75, 1669-1678 (1998)
14. Piston, D. W., M. S. Kirby, H. P. Cheng, W. J. Lederer & W. W. Webb: 2-photon-excitation fluorescence imaging of 3-dimensional calcium-ion activity. *Appl Optics* 33, 662-669 (1994)
15. Etter, E. F., M. A. Kuhn & F. S. Fay: Detection of changes in near-membrane  $\text{Ca}^{2+}$  concentration using a novel membrane-associated  $\text{Ca}^{2+}$  indicator. *J Biol Chem* 269, 10141-10149 (1994)
16. Blatter, L. A. & E. Niggli: Confocal near-membrane detection of calcium in cardiac myocytes. *Cell Calcium* 23, 269-279 (1998)
17. Eisner, D. A., W. J. Lederer & R. D. Vaughan-Jones: The quantitative relationship between twitch tension and intracellular sodium activity in sheep cardiac purkinje fibres. *J Physiol* 355, 251-266 (1984)
18. Leblanc, N. & J. R. Hume: Sodium current-induced release of calcium from cardiac sarcoplasmic reticulum. *Science* 248, 372-376 (1990)
19. Lipp, P. & E. Niggli: Sodium current-induced calcium signals in isolated guinea-pig ventricular myocytes. *J Physiol* 474, 439-446 (1994)
20. Lederer, W. J., E. Niggli & R. W. Hadley: Sodium-calcium exchange in excitable cells: Fuzzy space. *Science* 248, 283 (1990)
21. Wendt-Gallitelli, M. F., T. Voigt & G. Isenberg: Microheterogeneity of subsarcolemmal sodium gradients. Electron probe microanalysis in guinea-pig ventricular myocytes. *J Physiol* 472, 33-44 (1993)
22. Despa, S., L. A. Blatter, J. Kockskämper & D. M. Bers:  $[\text{Na}]_i$  imaging in rat ventricular myocytes using two-photon microscopy of SBF. *Biophys J* 84, 335a (2003)
23. Minta, A. & R. Y. Tsien: Fluorescent indicators for cytosolic sodium. *J Biol Chem* 264, 19449-19457 (1989)
24. Donoso, P., J. G. Mill, S. C. O'Neill & D. A. Eisner: Fluorescence measurements of cytoplasmic and mitochondrial sodium concentration in rat ventricular myocytes. *J Physiol* 448, 493-509 (1992)
25. Rose, C. R., Y. Kovalchuk, J. Eilers & A. Konnerth: Two-photon  $\text{Na}^+$  imaging in spines and fine dendrites of central neurons. *Pflügers Arch* 439, 201-207 (1999)
26. Rose, C. R. & A. Konnerth: NMDA receptor-mediated  $\text{Na}^+$  signals in spines and dendrites. *J Neurosci* 21, 4207-4214 (2001)
27. Eng, J., R. M. Lynch & R. S. Balaban: Nicotinamide adenine dinucleotide fluorescence spectroscopy and imaging of isolated cardiac myocytes. *Biophys J* 55, 621-630 (1989)
28. Griffiths, E. J., H. Lin & M. S. Suleiman: NADH fluorescence in isolated guinea-pig and rat cardiomyocytes exposed to low or high stimulation rates and effect of metabolic inhibition with cyanide. *Biochem Pharmacol* 56, 173-179 (1998)
29. Brandes, R., L. S. Maier & D. M. Bers: Regulation of mitochondrial  $[\text{NADH}]$  by cytosolic  $[\text{Ca}^{2+}]$  and work in trabeculae from hypertrophic and normal rat hearts. *Circ Res* 82, 1189-1198 (1998)
30. Perriott, L. M., T. Kono, R. R. Whitesell, S. M. Knobel, D. W. Piston, D. K. Granner, A. C. Powers & J. M. May: Glucose uptake and metabolism by cultured human skeletal muscle cells: Rate-limiting steps. *Am J Physiol Endocrinol Metab* 281, E72-80 (2001)
31. Isaeva, E. V. & N. Shirokova: Metabolic regulation of  $\text{Ca}^{2+}$  release in permeabilized mammalian skeletal muscle fibres. *J Physiol* 547, 453-462 (2003)
32. Piston, D. W., B. R. Masters & W. W. Webb: Three-dimensionally resolved NAD(P)H cellular metabolic redox imaging of the *in situ* cornea with two-photon excitation laser scanning microscopy. *J Microsc* 178, 20-27 (1995)
33. Patterson, G. H., S. M. Knobel, P. Arkhammar, O. Thastrup & D. W. Piston: Separation of the glucose-stimulated cytoplasmic and mitochondrial NAD(P)H responses in pancreatic islet beta cells. *Proc Natl Acad Sci U S A* 97, 5203-5207 (2000)
34. Maiti, S., J. B. Shear, R. M. Williams, W. R. Zipfel & W. W. Webb: Measuring serotonin distribution in live cells with three-photon excitation. *Science* 275, 530-532 (1997)
35. Tsien, R. Y: The green fluorescent protein. *Annu Rev Biochem* 67, 509-544 (1998)
36. Zhang, J., R. E. Campbell, A. Y. Ting & R. Y. Tsien: Creating new fluorescent probes for cell biology. *Nat Rev Mol Cell Biol* 3, 906-918 (2002)
37. Miyawaki, A., J. Llopis, R. Heim, J. M. McCaffery, J. A. Adams, M. Ikura & R. Y. Tsien: Fluorescent indicators for  $\text{Ca}^{2+}$  based on green fluorescent proteins and calmodulin. *Nature* 388, 882-887 (1997)

38. Demaurex, N. & M. Frieden: Measurements of the free luminal ER  $\text{Ca}^{2+}$  concentration with targeted "cameleon" fluorescent proteins. *Cell Calcium* 34, 109-119 (2003)
39. Fan, G. Y., H. Fujisaki, A. Miyawaki, R. K. Tsay, R. Y. Tsien & M. H. Ellisman: Video-rate scanning two-photon excitation fluorescence microscopy and ratio imaging with cameleons. *Biophys J* 76, 2412-2420 (1999)
40. Georget, M., P. Mateo, G. Vandecasteele, L. Lipskaia, N. Defer, J. Hanoune, J. Hoerter, C. Lagnier & R. Fischmeister: Cyclic AMP compartmentation due to increased cAMP-phosphodiesterase activity in transgenic mice with a cardiac-directed expression of the human adenylyl cyclase type 8 (ac8). *FASEB J* 17, 1380-1391 (2003)
41. Niggli, E: Localized intracellular calcium signaling in muscle: Calcium sparks and calcium quarks. *Annu Rev Physiol* 61, 311-335 (1999)
42. Adams, S. R. & R. Y. Tsien: Controlling cell chemistry with caged compounds. *Annu Rev Physiol* 55, 755-784 (1993)
43. Denk, W: Two-photon scanning photochemical microscopy: Mapping ligand-gated ion channel distributions. *Proc Natl Acad Sci USA* 91, 6629-6633 (1994)
44. Furuta, T., S. S. Wang, J. L. Dantzker, T. M. Dore, W. J. Bybee, E. M. Callaway, W. Denk & R. Y. Tsien: Brominated 7-hydroxycoumarin-4-ylmethyls: Photolabile protecting groups with biologically useful cross-sections for two photon photolysis. *Proc Natl Acad Sci USA* 96, 1193-1200 (1999)
45. Ellis-Davies, G. C. R., M. Matsukazi, A. Tachikawa, Y. Miyashita, M. Iino, R. Barsotti & H. Kasai: Development of caged glutamates for two-photon functional mapping of glutamate receptors in living hippocampal neurons. *Biophys J* 80, 344a-345a (2001)
46. Matsuzaki, M., G. C. R. Ellis-Davies, T. Nemoto, Y. Miyashita, M. Iino & H. Kasai: Dendritic spine geometry is critical for ampa receptor expression in hippocampal cal pyramidal neurons. *Nat Neurosci* 4, 1086-1092 (2001)
47. Lipp, P. & E. Niggli: Fundamental calcium release events revealed by two-photon excitation photolysis of caged calcium in guinea-pig cardiac myocytes. *J Physiol* 508, 801-809 (1998)
48. Soeller, C., M. D. Jacobs, P. J. Donaldson, M. B. Cannell, K. T. Jones & G. C. R. Ellis-Davies: Application of two-photon flash photolysis to reveal intercellular communication and intracellular  $\text{Ca}^{2+}$  movements. *J Biomed Opt* 8, 418-427 (2003)
49. Cheng, H., W. J. Lederer & M. B. Cannell: Calcium sparks: Elementary events underlying excitation-contraction coupling in heart muscle. *Science* 262, 740-744 (1993)
50. Wang, S. Q., L. S. Song, E. G. Lakatta & H. Cheng:  $\text{Ca}^{2+}$  signalling between single L-type  $\text{Ca}^{2+}$  channels and ryanodine receptors in heart cells. *Nature* 410, 592-596 (2001)
51. Lipp, P. & E. Niggli: Submicroscopic calcium signals as fundamental events of excitation-contraction coupling in guinea-pig cardiac myocytes. *J Physiol* 492, 31-38 (1996)
52. DelPrincipe, F., M. Egger & E. Niggli: Calcium signalling in cardiac muscle: Refractoriness revealed by coherent activation. *Nat Cell Biol* 1, 323-329 (1999)
53. Brown, E. B., J. B. Shear, S. R. Adams, R. Y. Tsien & W. W. Webb: Photolysis of caged calcium in femtoliter volumes using two-photon excitation. *Biophys J* 76, 489-499 (1999)
54. DelPrincipe, F., M. Egger, G. C. R. Ellis-Davies & E. Niggli: Two-photon and UV-laser flash photolysis of the  $\text{Ca}^{2+}$  cage, dimethoxynitrophenyl-EGTA-4. *Cell Calcium* 25, 85-91 (1999)
55. Albota, M. A., C. Xu & W. W. Webb: Two-photon fluorescence excitation cross sections of biomolecular probes from 690 to 960 nm. *Appl Optics* 37, 7352-7356 (1998)
56. Koester, H. J., D. Baur, R. Uhl & S. W. Hell:  $\text{Ca}^{2+}$  fluorescence imaging with pico- and femtosecond two-photon excitation: Signal and photodamage. *Biophys J* 77, 2226-2236 (1999)
57. Kiskin, N. I., R. Chillingworth, J. A. McCray, D. Piston & D. Ogden: The efficiency of two-photon photolysis of a "caged" fluorophore, o-1-(2-nitrophenyl) ethylpyranine, in relation to photodamage of synaptic terminals. *Eur Biophys J* 30, 588-604 (2002)
58. Hopt, A. & E. Neher: Highly nonlinear photodamage in two-photon fluorescence microscopy. *Biophys J* 80, 2029-2036 (2001)
59. Squirrell, J. M., D. L. Wokosin, J. G. White & B. D. Bavister: Long-term two-photon fluorescence imaging of mammalian embryos without compromising viability. *Nat Biotechnol* 17, 763-767 (1999)
60. Albota, M., D. Beljonne, J. L. Bredas, J. E. Ehrlich, J. Y. Fu, A. A. Heikal, S. E. Hess, T. Kogej, M. D. Levin, S. R. Marder, D. McCord-Maughon, J. W. Perry, H. Rockel, M. Rumi, G. Subramaniam, W. W. Webb, X. L. Wu & C. Xu: Design of organic molecules with large two-photon absorption cross sections. *Science* 281, 1653-1656 (1998)
61. Ventelon, L., S. Charier, L. Moreaux, J. Mertz & M. Blanchard-Desce: Nanoscale push-push dihydrophenanthrene derivatives as novel fluorophores for two-photon-excited fluorescence. *Angew Chem Int Ed Engl* 40, 2098-2101 (2001)

62. Adams, S. R., V. Lev-Ram & R. Y. Tsien: A new caged  $\text{Ca}^{2+}$ , azid-1, is far more photosensitive than nitrobenzyl-based chelators. *Chem Biol* 4, 867-878 (1997)
63. Larson, D. R., W. Zipfel, S. Clark, M. Bruchez, F. Wise & W. W. Webb: Novel water-soluble quantum-dots with large two-photon crosssections for biological imaging. *Biophys J* 84, 23a-23a (2003)
64. Medintz, I. L., A. R. Clapp, H. Mattoussi, E. R. Goldman, B. Fisher & J. M. Mauro: Self-assembled nanoscale biosensors based on quantum dot FRET donors. *Nat Mater* 2, 630-638 (2003)
65. Tokumasu, F. & J. Dvorak: Development and application of quantum dots for immunocytochemistry of human erythrocytes. *J Microsc* 211, 256-261 (2003)
66. Harkins, A. B., N. Kurebayashi & S. M. Baylor: Resting myoplasmic free calcium in frog skeletal muscle fibers estimated with fluo-3. *Biophys J* 65, 865-881 (1993)
67. Lakowicz, J. R., H. Szmajnski, K. Nowaczyk, W. J. Lederer, M. S. Kirby & M. L. Johnson: Fluorescence lifetime imaging of intracellular calcium in cos cells using Quin-2. *Cell Calcium* 15, 7-27 (1994)
68. French, T., P. T. So, D. J. Weaver, T. Coelho-Sampaio, E. Gratton, E. W. Voss & J. Carrero: Two-photon fluorescence lifetime imaging microscopy of macrophage-mediated antigen processing. *J Microsc* 185, 339-353 (1997)
69. Volkmer, A., V. Subramaniam, D. J. Birch & T. M. Jovin: One- and two-photon excited fluorescence lifetimes and anisotropy decays of green fluorescent proteins. *Biophys J* 78, 1589-1598 (2000)
70. Berney, C. & G. Danuser: FRET or no FRET: A quantitative comparison. *Biophys J* 84, 3992-4010 (2003)
71. Aspelmeyer, M., H. R. Bohm, T. Glatzer, T. Jennewein, R. Kaltenbaek, M. Lindenthal, G. Molina-Terriza, A. Poppe, K. Resch, M. Taraba, R. Ursin, P. Walther & A. Zeilinger: Long-distance free-space distribution of quantum entanglement. *Science* 301, 621-623 (2003)
72. Atatüre, M., A. V. Sergienko, B. E. Saleh & M. C. Teich: Dispersion-independent high-visibility quantum interference in ultrafast parametric down-conversion. *Phys Rev Lett* 84, 618-621 (2000)
73. Tanzilli, S., H. De Riedmatten, W. Tittel, H. Zbinden, P. Baldi, M. De Micheli, D. B. Ostrowsky & N. Gisin: Highly efficient photon-pair source using periodically poled lithium niobate waveguide. *Electron Lett* 37, 26-28 (2001)

**Key Words:** Ultrafast lasers, Confocal microscopy, Multi photon excitation, Cell physiology, Functional genomics, Calcium imaging, Green fluorescent protein, Review

**Send correspondence to:** Dr Ernst Niggli, Department of Physiology, University of Bern, Bülhlplatz 5, CH-3012 Bern, Switzerland, Tel: 41-31-631-8730, Fax: 41-31-631-4611, E-mail: [niggli@pyl.unibe.ch](mailto:niggli@pyl.unibe.ch), [www: http://beam.to/calcium\\_quark](http://beam.to/calcium_quark)